JACS
JOURNAL OF THE AMERICAN CHEMICAL SOCIETY

ARTICLE

pubs.acs.org/JACS

A Step toward the Wet Surface Chemistry of Glycine and Alanine on Cu{110}: Destabilization and Decomposition in the Presence of Near-Ambient Water Vapor

Andrey Shavorskiy,[†] Funda Aksoy,[‡,§] Michael E. Grass,[‡] Zhi Liu,[‡] Hendrik Bluhm,[∥] and Georg Held*[,†]

[†]Department of Chemistry, The University of Reading, Whiteknights, Reading, RG6 6AD, U.K.

[‡]Advanced Light Source, Lawrence Berkeley National Laboratory, Berkeley, California 94720, United States

[§]Department of Physics, Faculty of Arts and Sciences, Nigde University, Nigde, Turkey

[∥]Chemical Sciences Division, Lawrence Berkeley National Laboratory, Berkeley, California 94720, United States

Supporting Information

ABSTRACT: The coadsorption of water with organic molecules under near-ambient pressure and temperature conditions opens up new reaction pathways on model catalyst surfaces that are not accessible in conventional ultrahigh-vacuum surface-science experiments. The surface chemistry of glycine and alanine at the water-exposed Cu{110} interface was studied in situ using ambient-pressure photoemission and X-ray absorption spectroscopy techniques. At water pressures above 10^{-5} Torr a significant pressure-dependent decrease in the temperature for dissociative desorption was observed for both amino acids, accompanied by the appearance of a new CN intermediate, which is not observed for lower pressures. The most likely reaction mechanisms involve dehydrogenation induced by O and/or OH surface species resulting from the dissociative adsorption of water. The linear relationship between the inverse decomposition temperature and the logarithm of water pressure enables determination of the activation energy for the surface reaction, between 213 and 232 kJ/mol, and a prediction of the decomposition temperature at the solid−liquid interface by extrapolating toward the equilibrium vapor pressure. Such experiments near the equilibrium vapor pressure provide important information about elementary surface processes at the solid−liquid interface, which can be retrieved neither under ultrahigh vacuum conditions nor from interfaces immersed in a solution.

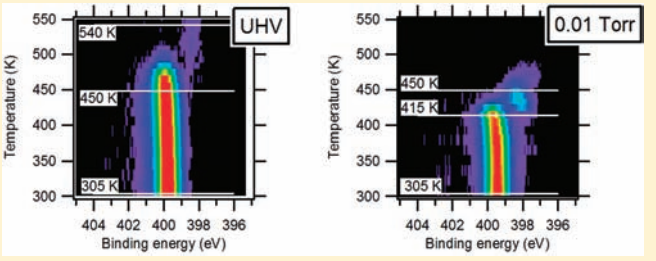

INTRODUCTION

The past decade has seen a dramatic increase in research into stereoselective heterogeneous catalysis of biorelated molecules, driven by the growing demand for environmentally friendly production methods for optically pure drugs using heterogeneous rather than homogeneous catalysts and, more recently, for biofuels from sources that are of no use for human or animal nutrition.[1−4] These new challenges require new classes of heterogeneous catalysts to avoid the problem of phase separation that is inherent to homogeneous catalytic processes in predominant use today.[5] Early examples of stereoselective heterogeneous catalysis are the enantioselective hydrogenation reactions of methyl pyruvate or methyl acetoacetate over chirally modified Pt or Ni catalysts, respectively.[6−8] In both cases, the catalyst surfaces are modified by chiral molecules, thus creating a reaction environment that favors the synthesis of one product enantiomer over the other.

The great challenge for fundamental surface science studies of model catalyst systems for biorelated heterogeneous reactions lies in the fact that practically all relevant reactions take place in solutions near room temperature. Such solution−catalyst interfaces are far less well understood than the catalyst interfaces for gas-phase reactions, because both solvent and reactants/modifiers interact at the solid surface and make the adsorption complex more complicated in many ways. Most surface science techniques require ultrahigh vacuum (UHV), but under these conditions water only forms stable condensed layers below 150 K,[9] which is far from realistic reaction conditions. At these temperatures both water and reactant molecules are much less mobile than at room temperature and the kinetic barriers for the key steps of the heterogeneously catalyzed reactions cannot be overcome: e.g., exchange of molecules between surface layer and solution or chemical reactions between the surface species. More realistic conditions can be achieved, however, when the catalyst interface is exposed to water vapor near the equilibrium vapor pressure, which is in the Torr range near room temperature. This "ambient pressure" range has recently become accessible for photoemission and X-ray absorption experiments through a new generation of differentially pumped detectors.[10−12] Some of the first experiments using these

Received: December 4, 2010
Published: April 07, 2011

dx.doi.org/10.1021/ja110910y | J. Am. Chem. Soc. 2011, 133, 6659–6667

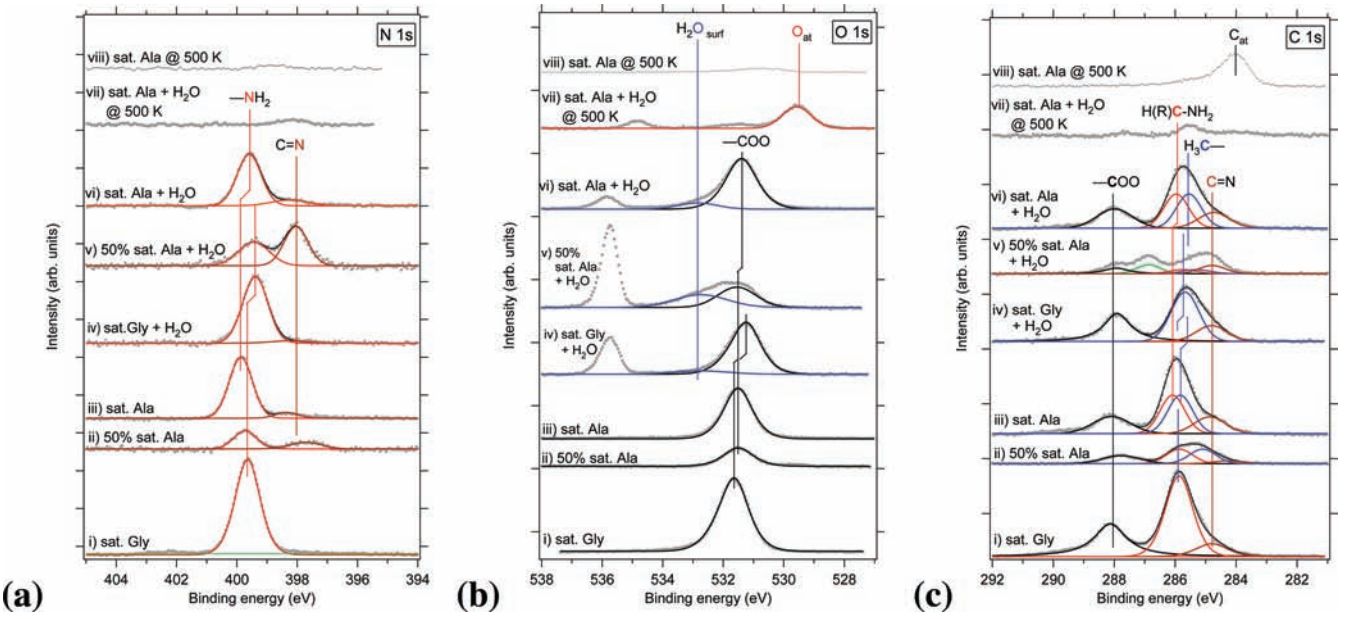

Figure 1. (a) N 1s (photon energy 510, 560 eV for ii and v), (b) O 1s (photon energy 650, 690 eV for ii and v) and (c) C 1s (photon energy 400, 450 eV for ii and v) XP spectra of glycine and alanine overlayers on Cu{110}: (i) 100% saturated glycine layer at 300 K in UHV; (ii) 50% saturated alanine layer at 300 K in UHV; (iii) 100% saturated alanine layer at 300 K in UHV; (iv) 100% saturated glycine layer at 300 K in 0.2 Torr H_2O atmosphere; (v) 50% saturated alanine layer at 266 K in 0.5 Torr H_2O atmosphere; (vi) 100% saturated alanine layer at 300 K in 0.1 Torr H_2O atmosphere; (vii) 50% saturated alanine layer at 420 K in 0.5 Torr H_2O atmosphere; (viii) 100% saturated alanine layer annealed to 500 K in UHV and 0.1 Torr H_2O atmosphere.

instruments showed that even the adsorption behavior of pure water can change dramatically, in comparison to UHV studies at temperatures below 150 K, when the pressure and temperature are raised to near-ambient conditions.[13−15]

Copper surfaces have become the model system of choice for fundamental surface science studies in the field of chiral modification. Typical chiral modifiers, such as small amino acids or tartaric acid, form well-ordered superstructures on these surfaces, which can be studied in detail with surface spectroscopic and crystallographic techniques (see ref 16 and references therein). This has led to important insights with respect to the relationship between molecular bonding and chiral expression on the molecular and macroscopic level.[17−21] One of the most studied substrates in this context is Cu{110}. In particular, the adsorption of glycine and alanine is well understood and it has been shown that the molecules chemisorb in their deprotonated form as glycinate and alaninate, forming surface bonds through the oxygen and nitrogen atoms.[22−30] Furthermore, the adsorption of water on Cu{110} has been studied in detail, both experimentally and theoretically. Below 165 K water adsorbs intact, whereas partial dissociation is observed above this temperature in UHV and ambient-pressure experiments.[13,31−40] For both layers, intact and partially dissociated, unusual hydrogen-bonded chain structures have been observed experimentally.[41,42] It was shown recently that Cu{110} is hydrophilic and is covered by a layer of OH + H_2O under ambient water pressure conditions (1 Torr) up to 500 K, whereas Cu{111} is hydrophobic under the same conditions.[13,14]

Here we present a study of the surface chemistry of chemisorbed layers of glycine and alanine on Cu{110} in the presence of water vapor up to the Torr range. Using X-ray photoelectron spectroscopy (XPS) and near-edge X-ray absorption fine structure (NEXAFS) spectroscopy, we find that the molecules change their chemical state if they are coadsorbed with partially dissociated water at around room temperature. The substrate bond is significantly weakened compared to the case for UHV conditions, and dissociative desorption occurs at temperatures up to 80 K lower than in UHV. These experiments clearly show that a solvent such as water will have a profound influence on any surface reaction involving such molecules and that relevant reaction mechanisms can only be found if biorelated reactants are studied under ambient relative humidity and temperature.

EXPERIMENTAL SECTION

The experiments were performed at the Advanced Light Source in Berkeley (Berkeley, CA) using beamlines 11.0.2 and 9.3.2. The endstations of both beamlines consist of two ultrahigh-vacuum (UHV) chambers with base pressures in the 10^{-10} Torr range, as described elsewhere.[11,43] The preparation chambers are equipped with standard instruments for sample preparation and characterization (sputter gun, LEED). The analysis chambers are dedicated to photoelectron spectroscopy at near-ambient-pressure conditions and were equipped with Specs Phoibos 150 (11.0.2) and Scienta 4000 HiPP (9.3.2) electron spectrometers, respectively, with custom-designed differentially pumped electron lenses,[44,45] which enable experiments up to water vapor pressures in the Torr range.

C 1s, N 1s, and O 1s XP spectra were recorded with excitation energies of 400/450, 510/560, and 650/690 eV, respectively, with a combined energy resolution of monochromator and electron analyzer between 0.3 and 0.6 eV. The offset of the binding energy (BE) scale was calibrated by recording spectra of the Fermi edge with the same beamline and analyzer settings as for the corresponding core levels. Temperature-programmed XP spectra (TP-XPS) are a series of fast XP spectra (typically 60 s per scan) recorded while the sample is heated at a rate of 0.10−0.17 K/s. All spectra were normalized with respect to the low-BE background, and a Shirley-type background[46] was subtracted prior to the peak fitting. The spectra were analyzed by fitting pseudo-Voigt peak shapes with additional exponential broadening at the high-BE

dx.doi.org/10.1021/ja110910y |J. Am. Chem. Soc. 2011, 133, 6659–6667

Table 1. Parameters of the Peaks Fitted to the XP Spectra in Figure 1

	C 1s		N 1s		O 1s	
surface species	BE (eV)	fwhm	BE (eV)	fwhm	BE (eV)	fwhm
			(i) Glycine (sat) UHV, Room Temperature			
−COO	288.1	1.2			531.6	1.2
$-H_2CNH_2$	286.1	1.0	399.6	1.0		
			(ii) Alanine (50% sat) UHV, Room Temperature			
−COO	287.8	1.4			531.4	1.2
$-MeHCNH_2$	285.8	1.0	399.7	0.9		
$-CH_3$	285.1	1.0				
H_xCN	284.3	1.1	397.7	1.2		
			(iii) Alanine (sat) UHV, Room Temperature			
−COO	288.1	1.4			531.5	1.1
$-MeHCNH_2$	286.1	1.0	399.9	0.9		
$-CH_3$	285.8	1.0				
H_xCN	284.9	1.2	398.3	0.9		
			(iv) Glycine (sat) 0.2 Torr H_2O, Room Temperature			
−COO	287.9	1.1			531.2	1.2
$-H_2CNH_2$	285.7	1.1	399.4	1.0		
H_xCN	284.8	1.2				
H_2O_{sur}					532.7	2.0
			(v) Alanine (50% sat) 0.5 Torr H_2O, 266 K			
−COO	287.9	1.0			531.6	1.5
	286.9	1.0				
$-MeHCNH_2$	285.7	1.0	399.4	1.2		
$-CH_3$	285.3	1.0				
H_xCN	284.8	1.2	398.0	0.9		
H_2O_{sur}					532.7	2.0
			(vi) Alanine (sat) 0.1 Torr H_2O, Room Temperature			
−COO	288.0	1.4			531.4	1.2
$-MeHCNH_2$	286.0	1.0	399.6	0.9		
$-CH_3$	285.5	1.0				
H_xCN	284.7	1.2	398.0	1.4		
H_2O_{sur}					532.8	1.5
			(vii) Alanine (sat) 0.1 Torr H_2O, 500 K			
O_{at}					529.5	1.1
			(viii) Alanine (sat) UHV, 500 K			
C_{at}	284.0	0.9				

side. The TP-XPS series were analyzed by linking certain parameters (fwhm, Gaussian−Lorentzian mixture, and asymmetry) for all spectra within the series.

NEXAFS spectra were recorded at the 11.0.2 endstation using the same analyzer as for XPS to measure the signal of carbon or nitrogen KLL Auger electrons at a kinetic energy of 270 or 406 eV, respectively. For the NEXAFS experiments the sample was oriented normal to the incident photon beam with the polarization vector either parallel or perpendicular to the close-packed rows of Cu atoms within the surface plane ([1$\bar{1}$0] or [001] direction). The spectra of the adsorbate-covered sample were normalized with respect to the clean-surface spectra in order to remove artificial features arising from X-ray absorption within the beamline, and a linear background was subtracted. The photon energy axis was calibrated such that the resonance features under UHV conditions coincide with those in previously published spectra.[23,29]

The Cu{110} surface was cleaned using standard procedures, including cycles of Ar^+ bombardment and annealing to 1000 K.[35] The sample temperature was monitored by a K-type thermocouple located at a sample holder which was in good thermal contact with the sample. Small amounts of residual carbon were removed by dosing 1×10^{-7} Torr of molecular oxygen at room temperature followed by annealing to 1000 K. The surface cleanliness was checked before each experiment by measuring survey spectra, and the impurity level (C, O, S) was always close to the XPS detection limit of less than 0.01 ML. Glycine and alanine were dosed via sublimation under vacuum from a home-built evaporation source at 150 °C, as described previously,[20] with the sample held at a temperature between 300 and 350 K.

Water was cleaned by several freeze−pump−thaw cycles and dosed through the background directly into the analysis chamber. At near-ambient pressures of water, even impurities at the 1 ppm level can

dx.doi.org/10.1021/ja110910y |J. Am. Chem. Soc. 2011, 133, 6659–6667

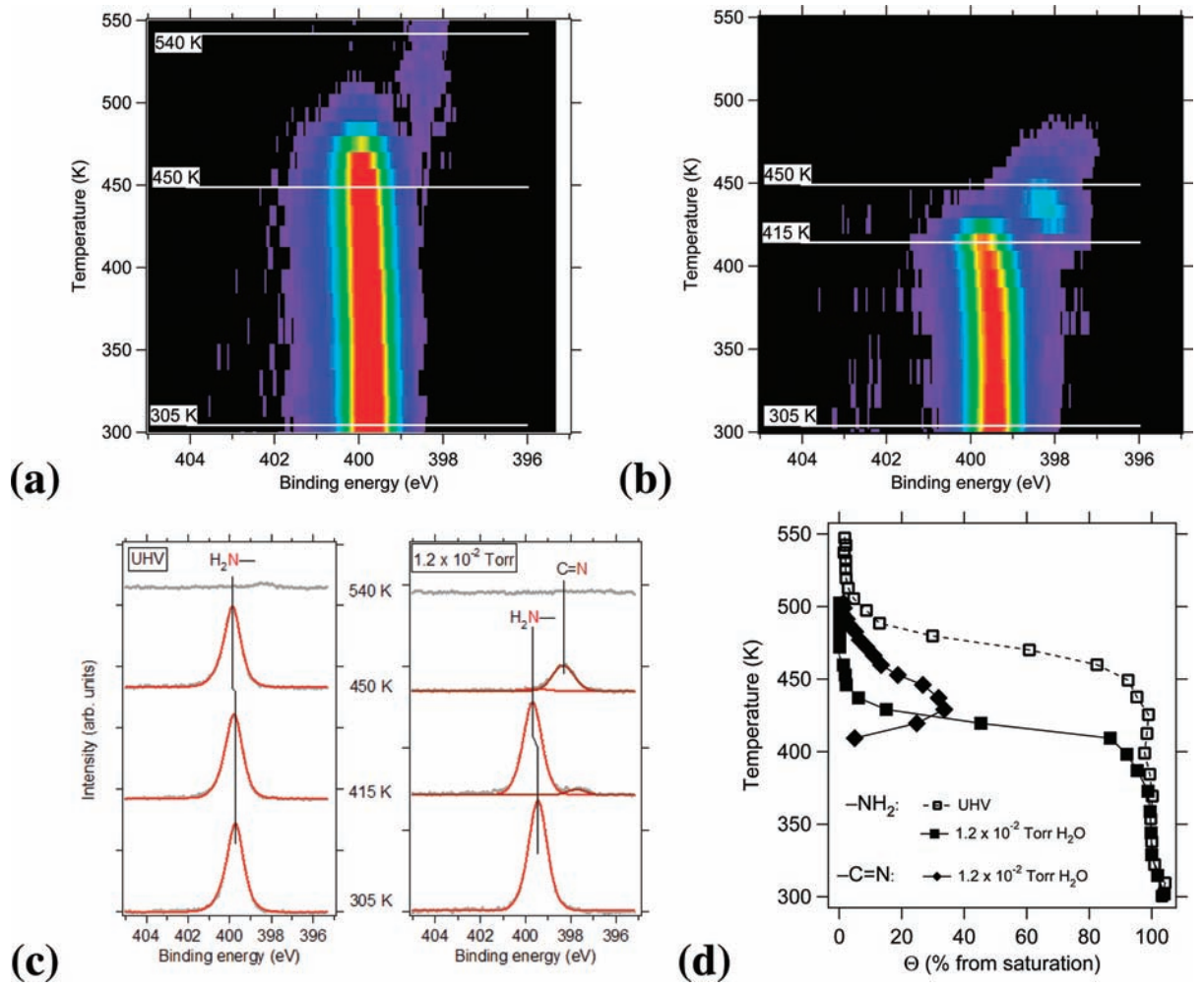

Figure 2. Series of N 1s TP-XPS (intensity versus binding energy and temperature) during annealing of a saturation layer of glycine on Cu{110} in (a) UHV and (b) in 1.2×10^{-2} Torr H_2O (heating rate ~0.17 K/s, 10 K/spectrum). (c) Single spectra taken from parts a and b. (d) Peak intensities (in percent of saturation coverage) vs sample temperature (photon energy 510 eV).

accumulate quickly on the surface. The main impurities found in our experiments were carbon- and sulfur-containing compounds. In order to maintain a low level of contamination, fast data acquisition was essential. We found that saturated chemisorbed amino acid layers prevent surface contamination with other species. Therefore, most of the experiments were carried out with saturated layers.

RESULTS

For comparison, XP spectra of chemisorbed layers of glycine (100% saturation; 0.33 mL) and alanine (50% and 100% saturation; 0.17 and 0.33 mL) on Cu{110} were recorded under UHV conditions at room temperature (see spectra i–iii in Figure 1a–c and Table 1). It was established in previous studies that both glycine and alanine lose the acidic hydrogen atom during adsorption at room temperature and form ordered chemisorbed layers of anionic glycinate and alaninate.[22,23,28,29,47] The observed O 1s and N 1s BEs around 531.5 and 400 eV, respectively, are typical for adsorption bonds through the two deprotonated oxygen atoms of the carboxylate group and the nitrogen atom of the amino group.[23,29] The C 1s spectra show two features around 288 and 286 eV, which are assigned to the carbon atom in the carboxylate group (−*C*OO) and the backbone/methyl carbon atoms ($C\mathrm{H_2NH_2}$ in glycine and $\mathrm{H_3}C\mathrm{CHNH_2}$ in alanine), respectively, in accordance with earlier studies.[23,29] The fact that the peak intensity of the carboxylate carbon is smaller than that expected from the stoichiometry for both molecules is in accordance with the earlier results and is most likely due to photoelectron diffraction. The small extra signal around BE 398 and 285 eV in the N 1s and C 1s spectra of alanine indicate some degree of dissociation leading to a CN surface species, which is more pronounced for the half-saturated layer than for the saturated layer (see spectra ii and iii in Figure 1a,c).

The N 1s region was chosen to monitor temperature and/or coadsorbate-induced changes because of its sensitivity to the chemical state of the molecules and the relative simplicity of the spectra. Figure 2a shows a TP-XPS series of N 1s spectra for the saturated chemisorbed layer of glycine under UHV conditions, which is almost identical with the corresponding alanine series (not shown). Individual key spectra are shown in the left panel of Figure 2c. All spectra of this TP-XPS series were fitted with a single peak, and the relative peak areas are plotted vs temperature in Figure 2d (open squares). At around 450 K the N 1s peak energy shifts by 0.2 eV toward higher BE while the intensity decreases. Above 510 K no more signal is observed around BE 400 eV; only a small signal due to decomposition

dx.doi.org/10.1021/ja110910y |*J. Am. Chem. Soc.* 2011, 133, 6659–6667

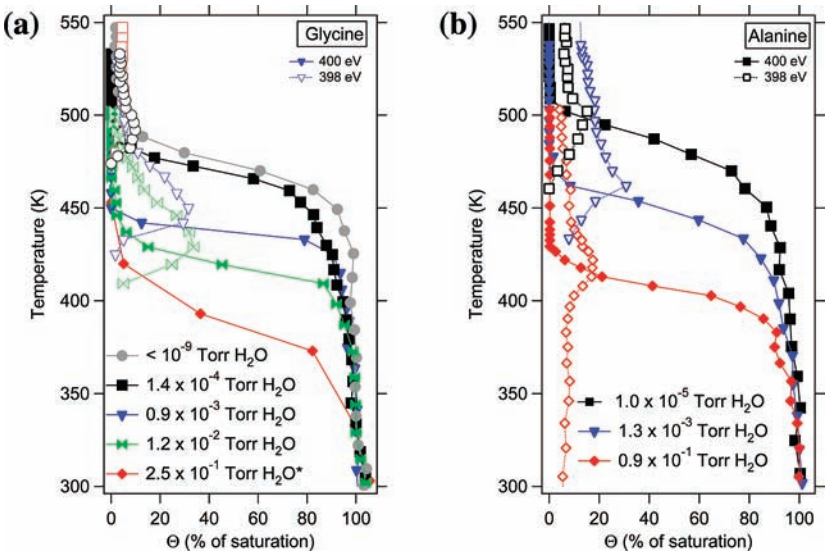

Figure 3. Areas of the N 1s peaks at BE 400 eV (filled markers) and BE 398 eV (open markers, both in percent of saturation coverage) as a function of sample temperature for saturated layers of alanine (a) and glycine (b) at various water pressures. The heating rate was 0.10−0.17 K/s between 400 and 500 K, except for the 2.5×10^{-1} Torr data of glycine, where the rate was 0.4 K/s. Note that the smaller number of data points in this curve leads to slightly different apparent slope in comparison to the other curves.

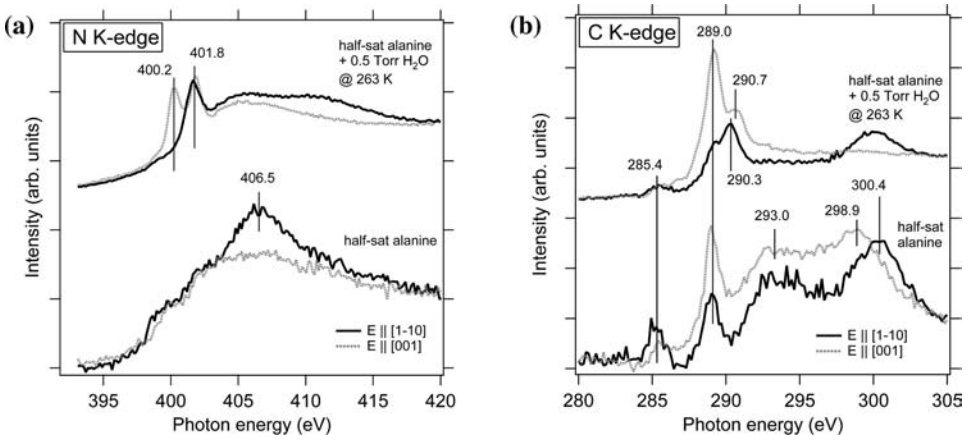

Figure 4. Nitrogen (a) and carbon (b) K-edge Auger-yield NEXAFS spectra recorded at normal incidence. The bottom spectra are those of a 50% saturation coverage of alanine on Cu{110} at 300 K. The top spectra are from the same layer exposed to 0.5 Torr H_2O at 266 K. Black solid lines denote polarization parallel to the $[1\bar{1}0]$ direction (parallel to close-packed rows of Cu atoms), and gray dotted lines denote polarization parallel to the [001] direction (perpendicular to close-packed rows of Cu atoms). The difference in noise levels between UHV and ambient-pressure data is due to different dwell times per data point.

products is measured at BE 398.5 eV, which is below 10% of the N 1s peak area of the saturated layer. The main decomposition product left on the surface under UHV conditions was atomic carbon for both glycine (20% of saturation signal, not shown) and alanine (50%, see Figure 1c, spectrum viii).

The temperature-induced behavior changes dramatically when the glycine or alanine layers are exposed to water vapor at pressures above 10^{-5} Torr. The TP-XPS series in Figure 2b shows changes in the N 1s region of the saturated glycine layer when annealed in water vapor of $p_{H_2O} = 1.2 \times 10^{-2}$ Torr; individual key spectra and relative peak areas are shown in Figure 2c (right panel) and Figure 2d (filled squares). The main N 1s peak starts decaying at 415 K, a much lower temperature than in the UHV series (Figure 2a), and a new peak appears around BE 398 eV, which is observed up to 480 K. The area of this peak is also included in Figure 2d (diamond-shaped data points); its maximum intensity is 35% of the N 1s signal at room temperature. In addition a new C 1s signal at BE 284.4 eV is observed (Figure 1c, spectra vi−vi), which shows the same temperature behavior as the N 1s peak at BE 398 eV. This coincidence together with further characterization by NEXAFS (see below) indicates that the two signals stem from a $(H_x)CN$ intermediate of the decomposition of the amino acids. Protonation of the amino group can be excluded as this would lead to an increase in the N 1s BE rather than the observed decrease.[21] Almost no N 1s or C 1s signal is observed above 500 K; the only significant peaks in the O 1s spectrum, at BE 535.0 and 529.5 eV, are associated with gas-phase water and atomic oxygen (cf. Figure 1a−c, spectra vii).

A series of similar experiments were performed for saturated chemisorbed layers of glycine and alanine on Cu{110} with

dx.doi.org/10.1021/ja110910y |J. Am. Chem. Soc. 2011, 133, 6659–6667

water vapor pressures ranging from 10^{-5} to 2.5×10^{-1} Torr. The results are summarized in Figure 3 by plots of the BE 400 eV and BE 398 eV N 1s peak areas vs temperature, which show a clear downward trend in the desorption temperature for increasing water pressure. This clearly identifies the presence of water at the surface as the origin of this effect. The midpoints of the steps in these plots define the maxima of the corresponding decomposition rate. They shift by 80 K for glycine between the 2.5×10^{-1} and 1.4×10^{-4} Torr curves and 75 K for alanine between the 0.9×10^{-1} and 1.0×10^{-5} Torr curves. The small difference between the UHV curve for glycine, which was measured at 10^{-9} Torr, and the curve for water vapor pressure of 1.4×10^{-4} Torr shows that the these effects are only significant above 10^{-5}–10^{-4} Torr. The maximum intensity of the N 1s peak at BE 398 eV is highest for pressures between 10^{-3} and 10^{-2} Torr, reaching 30–35% of the N 1s intensity of the saturated layer at 300 K.

Exposing saturated chemisorbed layers of glycine and alanine to water vapor in the 10^{-1} Torr range at room temperature does not lead to significant changes in the XPS features arising from the amino acids, as is illustrated in the corresponding spectra iv and vi of Figure 1a–c. The only effect of water on the N 1s, O 1s, and C 1s signals is a slight decrease in their BE by 0.15–0.30 eV. The new O 1s feature at BE 535.8 eV is the signal from gas-phase water. In addition a small intensity rise, equivalent to less than 0.10 ML, is observed around BE 533 eV, which arises from water molecules adsorbed on the saturated layers (Figure 1b).

The 50% saturation coverage of alanine exposed to 0.5 Torr water at 266 K, however, has about 0.40 ML of water present on the surface, covering most of the bare copper surface, as seen in the corresponding spectra v of Figure 1 a–c. The presence of coadsorbed water and/or its decomposition products (OH, O) leads to dramatic changes in the chemical state of alanine near room temperature. New peaks appear in the N 1s spectrum at BE 398.0 eV and in the C 1s spectrum at 286.9 eV, which are attributed to the products of the reaction between the alaninate surface species and water. This surface species was further characterized by NEXAFS. The nitrogen and carbon K-edge spectra for two orthogonal polarization angles are shown in parts a and b of Figure 4, respectively. The spectra at the bottom of Figure 4 are those of a layer of alanine at 50% saturation coverage under UHV conditions. They are in good agreement with spectra obtained previously for a saturated layer,[29] except for a smaller polarization dependence of the π resonance at 289.0 eV in the carbon spectra. This resonance is associated with the π^* orbital located at the carboxylate group. A change in the polarization dependence indicates changes in the azimuthal orientation of the molecules with respect to the saturated layer. The absence of strong pre-edge resonances in the N spectra implies that alanine is in its molecular form. The NEXAFS spectra change dramatically when water is added. Two new strong resonances appear at 400.2 and 401.8 eV in the N spectra and one around 290.5 eV in the C spectra (top spectra of Figure 4). In addition, the polarization dependence of the 289.0 eV resonance is much more pronounced than for the UHV spectra and coincides with the 400.2 eV resonance in the N spectra, whereas the resonances at 401.8 and 290.5 eV show almost no polarization dependence. Similar signatures in XPS and NEXAFS were observed previously for annealed layers of glycine and alanine on Pd{111}, Pt{111}, and Pt{110},[48–50] for HCN and CN species on Pd{111} and thick copper films,[51–53] and for other molecules with saturated and unsaturated C–N bonds.[54–56] Our data, therefore, suggest the presence of unsaturated C–N bonds, i.e. CN, HCN, or OCN, and thus partial decomposition of the molecules in the presence of water on the surface. The polarization dependence in NEXAFS implies that this adsorbed CN species has a well-defined orientation.

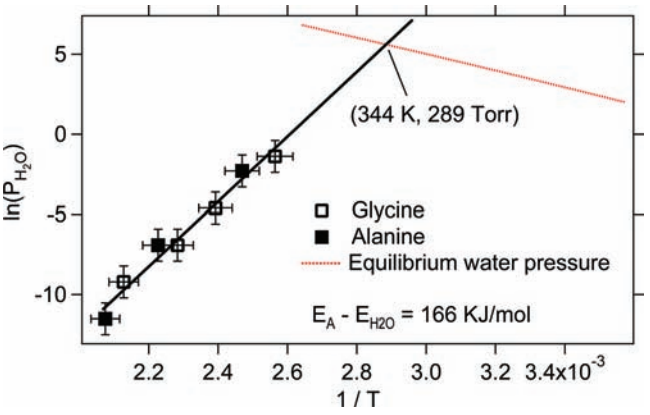

Figure 5. Plot of the logarithm of the H_2O vapor pressure vs the inverse desorption temperature of glycine (open squares) and alanine (filled squares). The desorption temperatures are defined by the midpoints of the steps in the intensity plots of Figure 2. The red dotted line indicates the temperature dependence of the equilibrium vapor pressure of water.

DISCUSSION

The most striking finding of the current study is the strong water vapor-pressure dependence of the amino acid decomposition temperature on Cu{110}. This effect is significant above 10^{-5} Torr and leads to a decrease in the decomposition/desorption temperature of around 80 K when the pressure rises to 10^{-1} Torr. From the present experimental data it is clear that the presence of water and/or its dissociation products at the surface is the key factor determining the temperature where decomposition and consecutive desorption of glycine or alanine takes place. When the surface is fully covered with glycine/alanine, only small amounts of water can condense on top of the molecular layer at 300 K and only small differences are observed with respect to the UHV data. Submonolayer coverages of alanine, however, allow the dissociative adsorption of a significant amount of water on the uncovered areas of the Cu{110} surface. Previous studies report dissociative adsorption of water on clean Cu{110}, with a surface OH species observed up to around 500 K when the surface is in equilibrium with near-ambient water vapor pressure.[13,15,35,36] The O 1s signal of coadsorbed water is significant in Figure 1b, spectrum v, for the half-saturated alanine layer exposed to 0.5 Torr. Coadsorbed water or its dissociation products induce the formation of a surface CN species even at room temperature, but this species desorbs only above about 400 K and appears to block the complete decomposition of the alanine layer at room temperature.

If the surface is fully covered with a layer of alanine or glycine and at a temperature above 400 K only small amounts of water are present at the surface. In this limit the water coverage, Θ_{H2O}, is proportional to the water partial pressure p_{H2O}:

$$\Theta_{H2O} = P_{H2O} \frac{\kappa}{\sqrt{2\pi m k_B T_{gas}}} \exp\left(\frac{E_{H2O}}{RT}\right) \qquad (1)$$

E_{H2O} is the adsorption energy of water, T the sample temperature (as opposed to T_{gas}), and κ a constant composed of the steric

dx.doi.org/10.1021/ja110910y |J. Am. Chem. Soc. 2011, 133, 6659–6667

factor for adsorption, the pre-exponential factor for desorption, and the area of the surface unit cell ($\kappa \approx 10^{-32}$ m^2 s). Assuming a simple Langmuir–Hinshelwood-type mechanism, the reaction rate can be expressed as

$$\frac{\mathrm{d}}{\mathrm{d}t}\Theta_{\mathrm{Gly/Ala}} = k\Theta_{\mathrm{Gly/Ala}}\Theta_{\mathrm{H2O}} = C\Theta_{\mathrm{Gly/Ala}}P_{\mathrm{H2O}}\exp\left(\frac{E_{\mathrm{H2O}} - E_{\mathrm{A}}}{RT}\right) \quad (2)$$

where C is the product of the pre-exponential factors of the rate constant k and the proportionality constant between gas pressure and adsorption rate ($\kappa/(2\pi m k_{\mathrm{B}} T_{\mathrm{gas}})^{1/2}$) and E_{A} the effective activation energy of the surface reaction. At the midpoints of the TP-XPS curves of Figure 3 all coverages, $\Theta_{\mathrm{Gly/Ala}}$, are the same (50% of saturation) and the reaction rates $(\mathrm{d}/\mathrm{d}t)\Theta_{\mathrm{Gly/Ala}}$ are of the same order of magnitude, as can be estimated from the slopes of the steps. Therefore, the logarithmic form of eq 2 can be rearranged as

$$\ln\left(\frac{P_{\mathrm{H2O}}}{P_0}\right) = \left(\frac{E_{\mathrm{A}} - E_{\mathrm{H2O}}}{R}\right)\frac{1}{T_{1/2}} + \mathrm{const} \quad (3)$$

and the difference between E_{H2O} and the effective activation energy of the surface reaction, E_{A}, can be obtained from the slope when plotting ln $P_{\mathrm{H_2O}}$ vs the inverse of the midpoint temperatures, $1/T_{1/2}$. Both glycine and alanine data line up on the same straight line (see Figure 5), whose slope corresponds to an activation energy difference of 166 ± 12 kJ/mol.[71] Considering that the experimental values for desorption energies of condensed and chemisorbed water, E_{H2O}, lie between 46.9 ± 0.9[57] and 66 ± 4.5 kJ/mol,[13] respectively, the value of the effective activation energy of the surface reaction, E_{A}, must be between 213 ± 12 and 232 ± 13 kJ/mol. This is significantly higher than the calculated activation energies for water dissociation (90 kJ/mol[40]) and glycine/alanine desorption (between 123 and 141 kJ/mol, depending on coverage[29,58]), which indicates that the decomposition is, indeed, a multistep process.

Equations 2 and 3 and Figure 5 imply that a lower water pressure can be compensated by an increase in the reaction temperature. At 10^{-5} Torr and below, however, a different, UHV decomposition path prevails, which does not require the presence of water. Using eq 1 (10^{-4} Torr, 475 K), we find a threshold water coverage is of the order of $10^{-5(\pm1)}$ ML. The first step of glycinate or alaninate decomposition in UHV involves breaking the backbone C_α–COO bond followed immediately by CO_2 desorption around 500 K, as observed in TPD.[28] The resulting methyl/ethylamine radicals (NH_2CH_2–) undergo several dehydrogenation and C–C bond cleavage reactions until hydrogen cyanide (HCN) is formed. Desorption of the latter species from Pt{111} was observed directly at around 500 K.[59] An alternative decomposition path for methylamine/ethylamine radicals is C–N bond cleavage followed by recombinative desorption of dinitrogen and C_xH_y species or complete dehydrogenation of hydrocarbon species. The latter leads to the formation of atomic carbon, which we have observed experimentally for both glycine and alanine layers on Cu{110} after annealing in UHV (cf. Figure 1 c, spectrum viii).

When the Cu{110} surface is in equilibrium with water vapor at near-ambient pressures, water, hydroxyl (atomic oxygen at elevated temperatures), and atomic hydrogen will be present at the surface.[13−15] Above 400 K these are short-lived intermediates, which cannot be observed directly. Surface O and/or OH can partially or fully oxidize both amino acids and their decomposition intermediates and thus open a new path for low-temperature decomposition. It has been shown that coadsorbed oxygen induces dehydrogenation of the amino groups of alkyl- and phenylamines on copper,[60−63] gold,[64] and silver[65] surfaces and can lead to the formation of nitriles via imides at room temperature. The surface reaction of alanine and glycine in the presence of water could therefore proceed as

$$\mathrm{COO{-}RCH{-}NH_2(a) + O(a) \xrightarrow{-H_2O} COO - RCH - N(a)} \quad (4a)$$

$$\mathrm{COO{-}RCH{-}NH_2(a) + OH(a) \xrightarrow{-H_2O,\,H_2} COO - RCH - N(a)} \quad (4b)$$

$$\mathrm{COO - RCH - N(a) \xrightarrow{-H_2,\,CO_2} HC{\equiv}N(+CH_x)} \quad (5)$$

The remaining surface species will undergo further C–H and C–N bond cleavage reactions induced by chemisorbed oxygen upon annealing, which lead to the formation of OH/H_2O, methane/ethylene/benzene, acetonitrile/cyanide, N_2 or CO/CO_2 (for detailed mechanisms see refs 61 and 64). All these reaction products desorb from copper surfaces immediately after formation when the sample temperature is above 400 K. Therefore, no residual carbon/nitrogen is left on the surface, in agreement with our experiments.

Hydrogen desorbs from Cu{110} around 325 K under UHV conditions but when produced between 400 and 500 K the dwell time at the surface is still of the order of milliseconds:[66] i.e., long enough to react with coadsorbed species. One possible reaction with hydrogen is the hydrogenation of the carboxylic groups of alaninate or glycinate, leading to recombinative desorption of intact molecules. An alternative reaction path would be the hydrogenation of methyl-/ethylamine radicals resulting from the initial CO_2–C_α bond cleavage[67−69] or even the formation of an intermediate H–C_α surface complex with the intact amino acid anions. The latter would lead to saturated amine products, which occupy a single adsorption site, in contrast to the two necessary for adsorption of the methyl-/ethylamine radicals. This significantly reduces steric constraints for the C–C bond cleavage and can, therefore, facilitate decomposition. The hydrogen reaction path can facilitate more or less immediate desorption after the reaction has taken place, but it is unlikely to lead to a CN species with a multiple-bond signature as observed in NEXAFS (cf. Figure 4). Therefore, on the basis of our experimental findings, oxygen- and/or hydroxyl-induced dehydrogenation appears to be the dominant decomposition mechanism. Further experiments with potential intermediates will be needed to elucidate the details of this mechanism.

Irrespective of the actual decomposition mechanism, it is important to note that the linear relationship between $\ln(P_{\mathrm{H2O}})$ and $1/T_{1/2}$ holds over 5 decades and can be extrapolated toward the equilibrium water vapor pressure,[70] which is indicated by the dotted (red) line in Figure 5. Above this pressure the surface is in equilibrium with liquid water; hence, the temperature at which the two curves intersect, 344 K (315 mbar/239 Torr), should correspond to the decomposition temperature of saturated chemisorbed alanine or glycine layers at the solid–liquid interface. With the N 1s signal at BE 398 eV of the CN decomposition

dx.doi.org/10.1021/ja110910y | J. Am. Chem. Soc. 2011, 133, 6659–6667

intermediate being unchanged over about 4 decades of water vapor pressure, from 10^{-5} to 10^{-1} Torr, we can assume that the rate-determining decomposition mechanism will continue to be the same up to the equilibrium vapor pressure. Ambient pressure measurements such as the above, therefore, enable us to characterize elementary reactions, which do not occur under UHV conditions but are important at the solid−liquid interface, despite the fact that the surface is not yet in contact with the liquid solvent phase. Further improvements in the experimental setup will probably allow the study of thin solvent films at reaction temperatures in the near future.

SUMMARY AND CONCLUSIONS

The surface chemistry of glycine and alanine on Cu{110} was studied by XPS and NEXAFS under ambient water pressure conditions. The presence of decomposition products of water (O, OH, H) at elevated temperatures (>400 K) opens up new reaction pathways, which lead to a significant decrease in the dissociative desorption temperature for both amino acids and the complete removal of carbonaceous species from the surface. The effect is significant for water pressures above 10^{-5} Torr and leads to a reduction in the decomposition temperature of up to 80 K at 10^{-1} Torr. Decomposition is accompanied by the observation of a CN intermediate, which is characterized by a shifted peak in the N 1s XP signal and sharp resonances in the N and C NEXAFS spectra. The most likely reaction mechanism involves oxygen- and/or hydroxyl-induced dehydrogenation of methyl-/ethylamine intermediates.

In the relevant pressure range we find a linear relationship between the inverse decomposition temperature and the logarithm of the water pressure. This relationship enables determining the activation energy for the surface reaction, at least 213 kJ/mol, and extrapolation toward the equilibrium vapor pressure to predict the decomposition temperature at the solid−liquid interface. Ambient-pressure measurements near the equilibrium vapor pressure can, therefore, be used to characterize elementary processes at the solid−liquid interface, which do not occur under UHV conditions, even though the surface is not yet in contact with the liquid solvent phase. These results clearly show that reaction mechanisms for heterogeneous reactions at the solution−solid interface cannot ignore the presence of solvent molecules at the surface, which makes their understanding and modeling far more complicated than gas-phase reactions.

ASSOCIATED CONTENT

Supporting Information. Text giving the complete ref 11. This material is available free of charge via the Internet at http://pubs.acs.org.

AUTHOR INFORMATION

Corresponding Author
*E-mail: g.held@reading.ac.uk.

ACKNOWLEDGMENT

This work was supported by the European Community through the Marie Curie Early Stage Training Network "MONET" (MEST-CT-2005-020908) and by the EPSRC through an overseas travel grant (No. EP/H015493/1). The Advanced Light Source is supported by the Director, Office of Science, Office of Basic Energy Sciences, of the U.S. Department of Energy under Contract No. DE-AC02-05CH11231.

REFERENCES

(1) Baiker, A. *J. Mol. Catal. A* **1997**, *115*, 473.
(2) Baiker, A. *J. Mol. Catal. A* **2000**, *163*, 205.
(3) Baddeley, C. *Top. Catal.* **2003**, *25*, 17.
(4) Baddeley, C. J.; Held, G. *Chiral Molecules on Surfaces*, 1st ed.; ; Elsevier: Amsterdam, 2010.
(5) Sharpless, K. *Angew. Chem., Int. Ed.* **2002**, *41*, 2024.
(6) Kean, M. A. *Langmuir* **1994**, *10*, 4560–4565.
(7) Kean, M. A. *Langmuir* **1997**, *13*, 41–50.
(8) Orito, Y.; Imai, S.; Nina, S. *J. Chem. Soc. Jpn.* **1979**, *8*, 1118.
(9) Henderson, M. A. *Surf. Sci. Rep.* **2002**, *46*, 1.
(10) Ogletree, D. F.; Bluhm, H.; Lebedev, G.; Fadley, C. S.; Hussain, Z.; Salmeron, M. *Rev. Sci. Instrum.* **2002**, *73*, 3872.
(11) Bluhm, H.; et al. *J. Electron Spectrosc. Relat. Phenom.* **2006**, *150*, 86.
(12) Salmeron, M.; Schlögl, R. *Surf. Sci. Rep.* **2008**, *63*, 169–199.
(13) Andersson, K.; Ketteler, G.; Bluhm, H.; Yamamoto, S.; Ogasawara, H.; Pettersson, L. G. M.; Salmeron, M.; Nilsson, A. *J. Phys. Chem. C* **2007**, *111*, 14493.
(14) Yamamoto, S.; Andersson, K.; Bluhm, H.; Ketteler, G.; Starr, D. E.; Schiros, T.; Ogasawara, H.; Pettersson, L. G. M.; Salmeron, M.; Nilsson, A. *J. Phys. Condens. Matt.* **2007**, *111*, 7848–7850.
(15) Andersson, K.; Ketteler, G.; Bluhm, H.; Yamamoto, S.; Ogasawara, H.; Pettersson, L. G. M.; Salmeron, M.; Nilsson, A. *J. Am. Chem. Soc.* **2008**, *130*, 2793.
(16) Barlow, S. M.; Raval, R. *Surf. Sci. Rep.* **2003**, *50*, 201.
(17) Forster, M.; Dyer, M. S.; Persson, M.; Raval, R. *J. Am. Chem. Soc.* **2009**, *131*, 10173–10181.
(18) Forster, M.; Dyer, M. S.; Persson, M.; Raval, R. *Angew. Chem.* **2010**, *49*, 2344–2348.
(19) Gladys, M. J.; Stevens, A. V.; Scott, N. R.; Jones, G.; Batchelor, D.; Held, G. *J. Phys. Chem. C* **2007**, *111*, 8331–8336.
(20) Eralp, T.; Zheleva, Z. V.; Shavorskiy, A.; Dhanak, V. R.; Held, G. *Langmuir* **2010**, *26*, 10918–10923.
(21) Eralp, T.; Shavorskiy, A.; Zheleva, Z. V.; Held, G.; Kalashnyk, N.; Ning, Y.; Linderoth, T. R. *Langmuir* **2010**, *26*, 18841–18851.
(22) Barlow, S. M.; Kitching, K. J.; Haq, S.; Richardson, N. V. *Surf. Sci.* **1998**, *401*, 322.
(23) Hasselström, J.; Karis, O.; Weinelt, M.; Wassdahl, N.; Nilsson, A.; Nyberg, M.; Petterson, L. G. M.; Samant, M. G.; Stöhr, J. *Surf. Sci.* **1998**, *407*, 221.
(24) Chen, Q.; Frankel, D. J.; Richardson, N. V. *Surf. Sci.* **2002**, *497*, 37.
(25) Rankin, R. B.; Sholl, D. S. *Surf. Sci.* **2004**, *548*, 301.
(26) Rankin, R. B.; Sholl, D. S. *Surf. Sci. Lett.* **2005**, *574*, L1.
(27) Rankin, R. B.; Sholl, D. S. *J. Phys. Chem. B* **2005**, *109*, 16764–16773.
(28) Barlow, S. M.; Louafi, S.; Le Roux, D.; Williams, J.; Muryn, C.; Haq, S.; Raval, R. *Surf. Sci.* **2005**, *590*, 243.
(29) Jones, G.; Jones, L. B.; Thibault-Starzyk, F.; Seddon, E. A.; Raval, R.; Jenkins, S. J.; Held, G. *Surf. Sci.* **2006**, *600*, 1924.
(30) Haq, S.; Massey, A.; Moslemzadeh, N.; Robin, A.; Barlow, S. M.; Raval, R. *Langmuir* **2007**, *23*, 10694–10700.
(31) Spitzer, A.; Lüth, H. *Surf. Sci.* **1982**, *120*, 376–388.
(32) Spitzer, A.; Lüth, H. *Surf. Sci.* **1985**, *160*, 353–361.
(33) Uy, P. S.; Bardolle, J.; Bujor, M. *Surf. Sci.* **1983**, *129*, 219–231.
(34) Bange, K.; Grider, D. E.; Madey, T. E.; Sass, J. K. *Surf. Sci.* **1984**, *136*, 38.
(35) Ammon, C.; Bayer, A.; Steinrück, H. P.; Held, G. *Chem. Phys. Lett.* **2003**, *377*, 163–169.
(36) Andersson, K.; Gòmez, A.; Glover, C.; Nordlund, D.; Öström, H.; Schiros, T.; Takahashi, O.; Ogasawara, H.; Pettersson, L. G. M.; Nilsson, A. *Surf. Sci. Lett.* **2005**, *584*, 183–189.

(37) Schiros, T.; Haq, S.; Ogasawara, H.; Takahashi, O.; Öström, H.; Andersson, K.; Pettersson, L. G. M.; Hodgson, A.; Nilsson, A. *Chem. Phys. Lett.* **2006**, *429*, 415.
(38) Tang, Q.-L.; Chen, Z.-X. *Surf. Sci.* **2007**, *601*, 954.
(39) Ren, J.; Meng, S. *J. Am. Chem. Soc.* **2006**, *128*, 9282–9283.
(40) Ren, J.; Meng, S. *Phys. Rev. B* **2008**, *77*, 054110.
(41) Lee, J.; Sorescu, D. C.; Jordan, K. D.; Yates, J. T., Jr. *J. Phys. Chem. C* **2008**, *112*, 17672.
(42) Carrasco, J.; Michaelides, A.; Forster, M.; Haq, S.; R., R.; Hodgson, A. *Nat. Mater.* **2009**, *8*, 427–431.
(43) Hussain, Z.; Huff, W. R. A.; Kellar, S. A.; Moler, E. J.; Heimann, P. A.; McKinney, W.; Padmore, H. A.; Fadley, C. S.; Shirley, D. A. *J. Electron Spectrosc. Relat. Phenom.* **1996**, *80*, 401.
(44) Bluhm, H. *J. Electron Spectrosc. Relat. Phenom.* **2010**, *177*, 71–84.
(45) Grass, M. E.; Karlsson, P. G.; Aksoy, F.; Lundqvist, M.; Wannberg, B.; Mun, B. S.; Hussain, Z.; Liu, Z. *Rev. Sci. Instrum.* **2010**, *81*, 053106.
(46) Shirley, D. *Phys. Rev. B* **1972**, *5*, 4709.
(47) Williams, J.; Haq, S.; Raval, R. *Surf. Sci.* **1996**, *368*, 303.
(48) Gao, F.; Li, Z.; Wanga, Y.; Burkholder, L.; Tysoe, W. T. *J. Phys. Chem. C* **2007**, *111*, 9981–9991.
(49) Gao, F.; Li, Z.; Wang, Y.; Burkholder, L.; Tysoe, W. T. *Surf. Sci.* **2007**, *601*, 3276–3288.
(50) Shavorskiy, A. Ph.D. Thesis, University of Reading, 2010
(51) Chen, J. J.; Winograd, N. *Surf. Sci.* **1995**, *326*, 285.
(52) Carley, A. F.; Chinn, M.; Parkinson, C. R. *Surf. Sci. Lett.* **2002**, *517*, L563.
(53) Carley, A. F.; Chinn, M.; Parkinson, C. R. *Surf. Sci.* **2003**, *537*, 64.
(54) Mitra-Kirtley, S.; Mullins, O. C.; van Elp, J.; George, S. J.; Chen, J.; Cramer, S. P. *J. Am. Chem. Soc.* **1993**, *115*, 252.
(55) Okajima, T.; Yamomoto, Y.; Ouchi, Y.; Seki, K. *J. Electron Spectrosc. Relat. Phenom.* **2001**, *114*−*116*, 849.
(56) Cook, P. L.; Xiaosong, L.; Yang, W.; Himpsel, F. J. *J. Chem. Phys.* **2009**, *131*.
(57) Speedy, R. J.; Debenedetti, P. G.; Smith, R. S.; Huang, C.; Kay, B. D. *J. Chem. Phys.* **1996**, *105*, 240–244.
(58) Blankenburg, S.; Schmidt, W. G. *Nanotechnology* **2007**, *18*, 424030.
(59) Kang, D.-H.; Trenary, M. *Surf. Sci.* **2002**, *519*, 40.
(60) Davies, P. R.; Shukla, N. *Surf. Sci.* **1995**, *322*, 8–20.
(61) Davies, P. R.; Edwards, D.; Richards, D. *Surf. Sci.* **2007**, *601*, 3253–3260.
(62) Prabhakaram, K.; Sen, P.; Rao, C. *Surf. Sci.* **1986**, *169*, L301–L306.
(63) Kelber, J.; Rogers, J. W., Jr.; Banse, B. A.; Koel, B. E. *App. Surf. Sci.* **1990**, *44*, 193–204.
(64) Gong, J.; Yan, T.; Mullins, C. B. *Chem. Commun.* **2009**, *2009*, 761–763.
(65) Thornburg, D.; Madix, R. J. *Surf. Sci.* **1990**, *226*, 61–76.
(66) Anger, G.; Winkler, A.; Rendulic, K. *Surf. Sci.* **1989**, *220*, 1–17.
(67) Maseri, F.; Peremans, A.; Darville, J.; Gilles, J. *J. Electron Spectrosc. Relat. Phenom.* **1990**, *54*−*55*, 1059–1064.
(68) Davies, P. R.; Keel, J. M. *Surf. Sci.* **2000**, *469*, 204–213.
(69) Chalker, S.; Haq, S.; Birtill, J. J.; T.S., N.; Raval, R. *Surf. Sci.* **2006**, *600*, 2364.
(70) Lide, D. R.; Frederikse, H. P. R. *Handbook of Chemistry and Physics*, 76th ed.; CRC Press: Boca Raton, FL, 1995.
(71) Only experimental errors were considered in the determination of the error margins; potential errors due to differences in the reaction rates $(d/dt)\Theta_{Gly/Ala}$ are not included.